Electronic structure of the $BaFe_2As_2$ family of iron-pnictide superconductors

M. Yi,[1,2] D. H. Lu,[1,2] J. G. Analytis,[3] J.-H. Chu,[3] S.-K. Mo,[2,4] R.-H. He,[1,2] R. G. Moore,[1,2] X. J. Zhou,[5] G. F. Chen,[5] J. L. Luo,[5] N. L. Wang,[5] Z. Hussain,[4] D. J. Singh,[6] I. R. Fisher,[3] and Z.-X. Shen[1,2,*]

[1]*SIMES, SLAC National Accelerator Laboratory, Menlo Park, California 94025, USA*

[2]*Geballe Laboratory for Advanced Materials, Departments of Physics and Applied Physics, Stanford University, Stanford, California 94305, USA*

[3]*Geballe Laboratory for Advanced Materials, Department of Applied Physics, Stanford University, Stanford, California 94305, USA*

[4]*Advanced Light Source, Lawrence Berkeley National Laboratory, Berkeley, California 94720, USA*

[5]*Institute of Physics, Chinese Academy of Science, Beijing 100080, China*

[6]*Materials Science and Technology Division, Oak Ridge National Laboratory, Oak Ridge, Tennessee 37831-6114, USA*

(Received 29 June 2009; published 24 July 2009)

We use high-resolution angle-resolved photoemission to study the electronic structure of the $BaFe_2As_2$ pnictides. We observe two electron bands and two hole bands near the X point, (π,π) of the Brillouin zone, in the paramagnetic state for electron-doped $Ba(Co_{0.06}Fe_{0.94})_2As_2$, undoped $BaFe_2As_2$, and hole-doped $Ba_{0.6}K_{0.4}Fe_2As_2$. Among these bands, only the electron bands cross the Fermi level, forming two electron pockets around X while the hole bands approach but never reach the Fermi level. We show that the band structure of the $BaFe_2As_2$ family matches reasonably well with the prediction of local-density approximation calculations after a momentum-dependent shift and renormalization. Our finding resolves a number of inconsistencies regarding the electronic structure of pnictides.

DOI: 10.1103/PhysRevB.80.024515 PACS number(s): 74.25.Jb, 74.70.−b, 79.60.−i

One reason the pnictides have captured and retained so much attention in the high-T_c field is the complexity of its electronic structure and the many mysteries that still remain unsolved. The undoped parent compound, $BaFe_2As_2$, exhibits a spin-density-wave (SDW) ordering,[1–3] which is suppressed with doping leading to superconductivity.[4–7] It has been suggested based on local-density approximation (LDA) calculations that the SDW results from nesting of the holelike Fermi surface (FS) at Γ and electronlike FS at X.[8,9] However, angle-resolved photoemission spectroscopy (ARPES) reports so far do not converge on the electronic structure at the X point,[10–18] and also appear to be inconsistent with LDA calculations, painting a different picture from earlier work on other pnictide compounds.[19] Given the complexity of the multiband nature of the material, it is important to understand the basic character of the band structure before more subtle many-body physics can be understood.

In this paper, we present a detailed high-resolution ARPES study to clarify the electronic structure around the X point in the $BaFe_2As_2$ family in the paramagnetic state. At temperatures above all transitions, we resolve two electron bands that cross the Fermi level (E_F) and two hole bands that approach but remain below E_F. Furthermore, from a series of cuts across the region at the Brillouin-zone (BZ) boundary near X, we observe that the electron and hole bands hybridize with a sizable gap in the region away from the Γ-X high-symmetry line, the details of which are well captured by nonmagnetic LDA calculations after a momentum-dependent shift and bandwidth renormalization, in contrast to the interpretation of a recent ARPES report.[15] The origin of this shift could be due to either a subtle surface issue or the limitation of the nonmagnetic LDA calculation. Finally, with measurements on $BaFe_2As_2$, $Ba_{0.6}K_{0.4}Fe_2As_2$, and $Ba(Co_{0.06}Fe_{0.94})_2As_2$, we show that such a band-structure character at X is general in the $BaFe_2As_2$ family across both electron and hole doping regimes. Our findings resolve a number of inconsistencies and provide a coherent picture on the electronic structure of pnicides.

High-quality single crystals of $Ba_{0.6}K_{0.4}Fe_2As_2$ (T_c=37 K) (Ref. 20), $BaFe_2As_2$, and $Ba(Co_{0.06}Fe_{0.94})_2As_2$ (T_c=25 K) (Ref. 7) were all grown using the self-flux method. ARPES measurements were taken at ALS beamline 10.0.1 and SSRL beamline 5–4, with an energy resolution better than 16 meV and angular resolution of 0.3°. All samples were cleaved *in situ* at various temperatures discussed below and measured under a base pressure $<4\times10^{-11}$ torr.

The parent compound $BaFe_2As_2$ undergoes both an SDW and structural transition at T_{SDW}=137 K. The electronic structure at low temperatures is more complex due to the presence of the SDW, which will be discussed in another paper. In this paper, we focus on the electronic structure in the paramagnetic state above T_{SDW} in comparison with nonmagnetic LDA. A FS intensity map of $BaFe_2As_2$ taken at 140 K is shown in Fig. 1(b). Figure 1(a) shows energy distribution curves (EDCs) along the high-symmetry cut Γ-X. At Γ, there is a clear holelike dispersion which forms a circular hole pocket on the FS, in agreement with LDA.[9,21] At X, surprisingly, there also appears to be a holelike dispersion and a cross-shaped FS which may seem to be in contradiction with the two electron pockets predicted by LDA, as also reported by other ARPES measurements.[10–18] However, as a more systematic comparison between the calculated band structure and experimental data in the region near X would show, LDA does not fail as miserably as it has been proclaimed.[15]

Let us first take a closer look at the LDA band structure calculated for the paramagnetic state around the X point. Besides two electron bands (e_1,e_2), there are also two hole bands (h_1,h_2) at higher binding energies [Fig. 1(c)]. The lower electron band e_2 intersects both hole bands and the upper electron band e_1 meets the upper hole band h_1 at X.

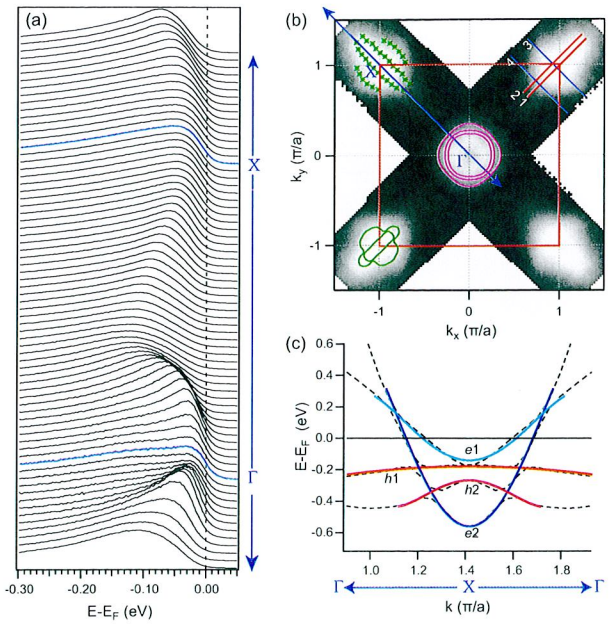

FIG. 1. (Color online) Measurements on $BaFe_2As_2$ taken at 140 K ($h\nu$=40 eV). (a) EDCs along the high-symmetry line Γ-X marked in (b). (b) Symmetrized FS map. The red square bounded by −1 to 1 in k_x and k_y marks the 1st BZ. Top left quadrant shows in green dots the outline of the electron pockets obtained from k_F points. Green and magenta lines mark the LDA calculated electron and hole pockets at X and Γ, respectively, after a nonuniform shift of E_F (down by 0.14 eV at X and up by 0.01 eV at Γ). (c) LDA bands near X along the Γ-X-Γ direction shown in dashed lines, resulting from hybridization of two hole band (h_1,h_2) and two electron bands (e_1,e_2).

The hybridization between h_1 and e_2 is forbidden by symmetry along the exact high-symmetry line Γ-X. However, away from Γ-X, the hybridization between these two bands strengthens with a sizable gap opening up in the band dispersions. These results imply strong angle-dependent variation in the orbital character between xz/yz and xy on the electron FS at X.

Shown in Fig. 2 are selected cuts around the X point, two cuts parallel and two cuts perpendicular to the Γ-X direction. For a better comparison, we superimpose LDA calculations on top of ARPES spectra after a downward E_F shift of 0.14 eV and a bandwidth renormalization of a factor of 1.5 [Figs. 2(b) and 2(c)]. Along the Γ-X high-symmetry line (cut 1), ARPES spectra are dominated by a flat holelike dispersion. As we go off the high-symmetry line (cut 2), the holelike dispersion clearly breaks into three segments with a higher middle segment. This effect strengthens away from the high-symmetry line (not all shown) and is exactly predicted by LDA calculations as the e_2 band hybridizes with the h_1 band. Along the high-symmetry cut perpendicular to Γ-X (cut 3), we see evidence for two electron bands that cross E_F and the top of a holelike band in between, corresponding to the e_1, e_2, and h_2 bands in LDA. The weaker e_2 and h_2 bands are more evident in the second derivative plot (row c) and the momentum distribution curve (MDC) plot (row d). As we move away from the high-symmetry cut (cut 4), the e_1 band gradually disappears above E_F while the e_2 and h_2 bands shift upward, as expected from LDA calculations. Overall, a good agreement can be found between calculated bands and experimental data, including the character (electron or hole) and relative locations of the bands.

One of the reasons that LDA calculation was dismissed as a plausible interpretation in previous ARPES studies[15] was

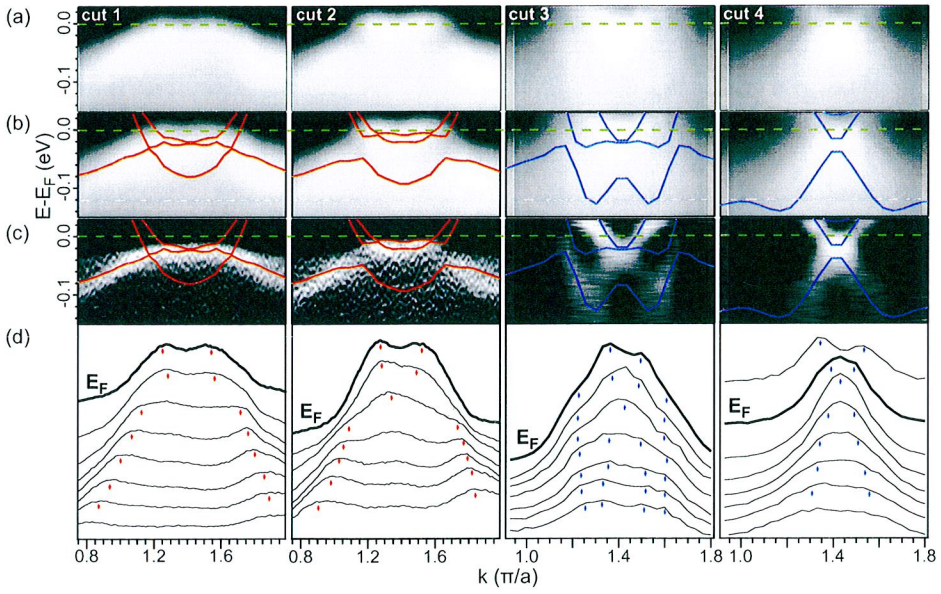

FIG. 2. (Color online) Spectra of $BaFe_2As_2$ taken at 140 K ($h\nu$=40 eV) along cuts near X, with positions labeled in Fig. 1(b). The light polarization is perpendicular to the Γ-X direction in all cuts. (a) Spectra divided by the Fermi-Dirac function to reveal band dispersions above E_F. (b) LDA bands ($k_z=\pi$) (Ref. 22) overlaid on corresponding cuts in (a) after a shift of E_F down by 0.14 eV and a bandwidth renormalization of a factor of 1.5. (c) Second derivative plots of (a), overlaid with LDA bands. (d) MDCs of (a) for the corresponding cuts, marking band dispersions.

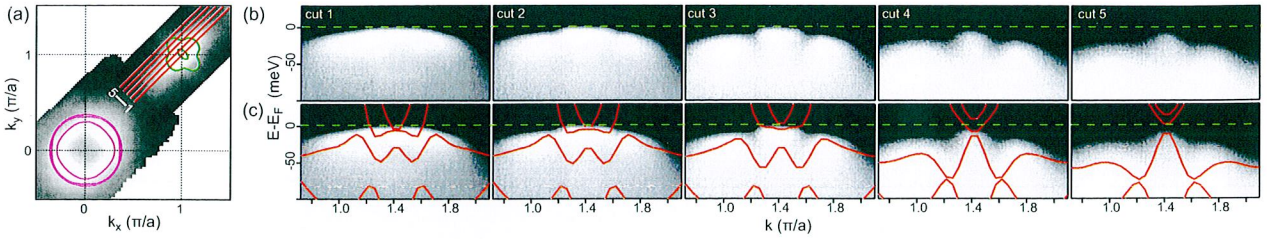

FIG. 3. (Color online) Spectra of $Ba_{0.6}K_{0.4}Fe_2As_2$ (T_c=37 K) taken at 45 K ($h\nu$=27 eV). (a) FS maps around Γ and X, overlaid with LDA FS (k_z=0) (Ref. 22) calculated for $Ba_{0.6}K_{0.4}Fe_2As_2$ after a shift of E_F down by 0.09 eV at X and no shift at Γ. (b) Spectra along parallel cuts marked in (a). (c) LDA bands (k_z=0) for corresponding cuts, (see text).

the failure to observe two electron bands near the X point. The reason that e_2 is only visible in the cut perpendicular to the Γ-X direction is likely due to a combination of its orbital symmetries, light polarization, and k_z dispersion. Note that all cuts shown in Fig. 2 were taken with an in-plane light polarization perpendicular to the Γ-X direction, which defines a mirror plane (xz plane in the single-Fe unit cell). Since the light polarization is odd with respect to this mirror plane, bands of even orbital symmetries with respect to this mirror plane (d_{xz}, $d_{x^2-y^2}$, and d_{z^2}) would be suppressed along this high-symmetry line. Therefore, e_2 could have one of these orbital symmetries. We note that the observation of two electron bands and hence two electron pockets around X has also been reported in a sister compound $SrFe_2As_2$ (Ref. 17). Therefore, this appears to be general to all undoped 122 parent compounds and can be understood in the framework of LDA calculations.

The comparison with LDA also helps us to understand the FS topology at X. As shown in the cuts parallel to the Γ-X direction (cuts 1 and 2 in Fig. 2), h_1 approaches but never crosses E_F. This can also be confirmed in the cuts perpendicular to the Γ-X direction (cuts 3 and 4 in Fig. 2). LDA shows that the e_1-band bottom touches the h_1-band top. Figure 2 shows that the e_1-band bottom is clearly below E_F, suggesting that the h_1-band top stays below E_F. Hence at X, only the two electron bands cross E_F, forming two electron pockets centered at X. In Fig. 1(b), the top left quadrant shows the outlines of the electron pockets determined from k_F points (momenta at which bands cross E_F). The two electron pockets hybridize to form an outer pocket and an inner pocket. Using the same downward E_F shift of 0.14 eV, we obtain an LDA FS topology quite comparable to the measurement at X, as shown in the lower left quadrant in Fig. 1(b). We should also point out that a very small E_F shift of 0.01 eV upward is needed at Γ to match the experimental FS. LDA predicts three nearly degenerate hole bands at Γ that cross E_F, which cannot be resolved from our data. Assuming this threefold degeneracy, we obtain a total holelike area of 2.7%×3=8.1% of the BZ at Γ and a total electronlike area of 6.9% of the BZ at X. This amounts to a Luttinger volume of 0.02 electrons per BZ, very close to the nominal doping level for undoped $BaFe_2As_2$ within experimental uncertainties, in sharp contrast to the much larger discrepancy of nearly one electron in LaOFeP.[19]

The agreement between experimental data and LDA calculations is not limited to the parent compound. In Figs. 3 and 4, we show similar measurements on hole-doped $Ba_{0.6}K_{0.4}Fe_2As_2$ and electron-doped $Ba(Co_{0.06}Fe_{0.94})_2As_2$. Both are optimally doped so that the SDW and structural transitions are suppressed.[7,20] Measurements were taken in their respective normal states above T_c. A series of cuts parallel to the Γ-X direction for $Ba_{0.6}K_{0.4}Fe_2As_2$ [Fig. 3(b)] clearly shows the holelike dispersion breaking into three segments as it hybridizes with the electron band away from Γ-X. The electron bands are again suppressed in this polarization geometry and only appear in the perpendicular cuts (not shown) as in $BaFe_2As_2$. Moreover, the center piece is always above the side pieces, yet always remains below E_F. Hence, even in the optimally hole-doped compound, we confirm that only the electron bands cross E_F, resulting in two electron pockets at X. Again, LDA calculated for $Ba_{0.6}K_{0.4}Fe_2As_2$ can match measured band dispersions in the region across X well after shifting E_F down by 0.09 eV and renormalizing by a factor of 2.7 [Fig. 3(c)]. It is interesting to note that the renormalization effect is stronger in this compound near optimal doping. Figure 3(a) shows LDA FS with a downward

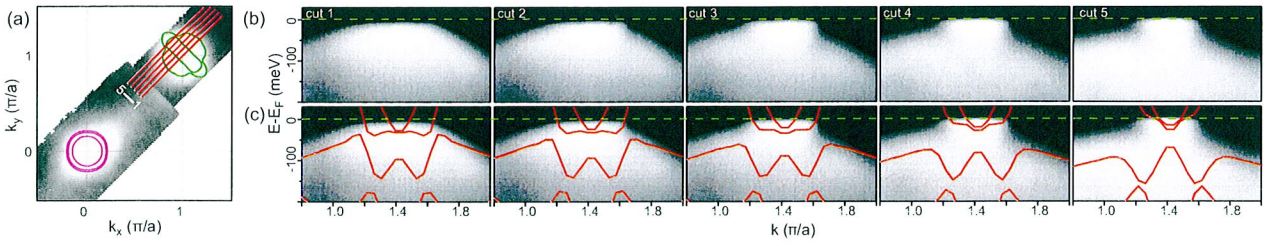

FIG. 4. (Color online) Spectra of $Ba(Co_{0.06}Fe_{0.94})_2As_2$ (T_c=25 K) taken at 35 K ($h\nu$=25 eV). (a) Measured FS, overlaid with LDA FS (k_z=0) calculated for $BaFe_2As_2$ after a shift of E_F down by 0.13 eV at X and up by 0.03 eV at Γ. (b) Spectra along cuts marked in (a). (c) LDA bands (k_z=0) for the corresponding cuts, (see text).

E_F shift of 0.09 eV at X and no shift at Γ, overlaid on measured FS.

Similarly, Fig. 4(b) shows a series of cuts parallel to the Γ-X direction for $Ba(Co_{0.06}Fe_{0.94})_2As_2$. Again, we see a nearly complete hole band on the high-symmetry cut and strongly hybridized pieces off the high-symmetry line. The center piece is lower than both the undoped and hole-doped compounds as we can see more of the electron pocket below E_F, consistent with electron doping. Since the doping for this compound is quite small, we compare its band dispersions with undoped LDA, in Fig. 4(c), where E_F is shifted down by 0.13 eV and renormalized by a factor of 1.4. Overlaid on the measured FS in Fig. 4(a) is LDA FS after an E_F shift down by 0.13 eV at X and up by 0.03 eV at Γ.

Comparing across all three dopings, we see that the hole pockets at Γ indeed becomes smaller toward electron doping as expected. At X, since many bands hybridize close to E_F, the FS topology changes more dramatically with doping. But overall, the degree (number of bands, band character, and hybridization effects) to which a simply shifted and renormalized LDA band structure can match well with measured band dispersion through a wide doping range in the $BaFe_2As_2$ family is remarkable, suggesting that LDA can capture the essential physics in these compounds. The next step is to understand the origin of the momentum-dependent shift to obtain such a match. One possibility is that the lack of natural cleavage plane in these crystals causes atoms on the cleaved surface to relax, perturbing the Fe-As bond angle, which is found to be important in setting the electronic structure in these compounds.[23] Alternatively, such a momentum-dependent shift could also be due to the limitation of a simple LDA calculation. For example, in the parent compound, it might be possible that residual short-range magnetic ordering in the paramagnetic phase and associated k-dependent spin fluctuations shift the relevant bands, which is not taken into account in the nonmagnetic LDA calculations. While this subtle discrepancy may hint at important physics, an ultimate understanding of this puzzling issue would require further efforts from both theoretical and experimental sides.

The results we have presented resolve a number of inconsistencies in the interpretation of previous ARPES results on the 122 pnictides. LDA predicts two electron pockets at X (Ref. 9) but previous ARPES papers have reported intensity spots[13] or a holelike propeller shape at X.[15] Since h_1 is very flat and close to E_F, it would contribute high intensity in the integration window when making a FS map, especially if resolution is considered. Furthermore, in doped samples below T_c, the superconducting gap would gap out spectral weight of the hybridized electron pocket that crosses E_F, effectively increasing the relative contribution of h_1, resulting in the appearance of holelike propeller-shaped FS pieces, even though this band does not cross E_F. Hence, it is important to map out the FS above T_c to avoid such complications. It has also been proposed that a folding between Γ and X results in a gap between electron and hole bands at X.[15] However, as we have shown, the gap mentioned in that work could be alternatively interpreted as simple electron and hole-band hybridization predicted by LDA, which is stronger away from the high-symmetry line. The degree to which shifted and renormalized LDA calculation matches measured band dispersion even away from the high-symmetry line strongly suggests that this is a simple band-structure feature rather than more complicated many-body effects.

In summary, we have observed in the paramagnetic state two hole bands and two electron bands at X that are common features in the $BaFe_2As_2$ family. The hole bands approach but remain below E_F while the electron bands cross E_F, forming two electron pockets as the only FS sheets at X. Moreover, we found that the hole bands hybridize with one of the electron bands away from the Γ-X high-symmetry line. Although more work is needed to fully understand the origin of the momentum-dependent shift and renormalization, the degree to which details in the LDA can capture the measured band dispersion and FS topology across doping regimes in ARPES data up to date suggest that this is the most appropriate and comprehensive interpretation which provides a consistent picture for the electronic structure of pnictides.

ACKNOWLEDGMENTS

We thank I.I. Mazin, Y. Yin, H. Yao, W.S. Lee, and B. Moritz for helpful discussions. This work is supported by the U.S. DOE, Office of Basic Energy Sciences at ALS (Grant No. DE-AC02-05CH11231), SSRL, Stanford University (Grant No. DE-AC02-76SF00515), and at ORNL. M.Y. thanks the NSF Graduate Research Fellowship for support.

*zxshen@stanford.edu

[1] M. Rotter, M. Tegel, D. Johrendt, I. Schellenberg, W. Hermes, and R. Pottgen, Phys. Rev. B **78**, 020503(R) (2008).

[2] C. de la Cruz, Q. Huang, J. W. Lynn, J. Li, W. Ratcliff II, J. L. Zarestky, H. A. Mook, G. F. Chen, J. L. Luo, N. L. Wang, and P. Dai, Nature (London) **453**, 899 (2008).

[3] Q. Huang, Y. Qiu, Wei Bao, M. A. Green, J. W. Lynn, Y. C. Gasparovic, T. Wu, G. Wu, and X. H. Chen, Phys. Rev. Lett. **101**, 257003 (2008).

[4] M. Rotter, M. Tegel, and D. Johrendt, Phys. Rev. Lett. **101**, 107006 (2008).

[5] H. Chen, Y. Ren, Y. Qiu, W. Bao, R. H. Liu, G. Wu, T. Wu, Y. L. Xie, X. F. Wang, Q. Huang, and X. H. Chang, EPL **85**, 17006 (2009).

[6] N. Ni, M. E. Tillman, J.-Q. Yan, A. Kracher, S. T. Hannahs, S. L. Bud'ko, and P. C. Canfield, Phys. Rev. B **78**, 214515 (2008).

[7] J.-H. Chu, J. G. Analytis, C. Kucharczyk, and I. R. Fisher, Phys. Rev. B **79**, 014506 (2009).

[8] J. Dong, H. J. Zhang, G. Xu, Z. Li, G. Li, W. Z. Hu, D. Wu, G. F. Chen, X. Dai, J. L. Luo, Z. Fang, and N. L. Wang, EPL **83**, 27006 (2008).

[9] D. J. Singh, Phys. Rev. B **78**, 094511 (2008).

[10] L. X. Yang, Y. Zhang, H. W. Ou, J. F. Zhao, D. W. Shen, B. Zhao, J. Wei, F. Chen, M. Xu, C. He, Y. Chen, Z. D. Wang, X. F. Wang, T. Wu, G. Wu, X. H. Chen, M. Arita, K. Shimada, M. Taniguchi, Z. Y. Lu, T. Xiang, and D. L. Feng, Phys. Rev. Lett. **102**, 107002 (2009).

[11] C. Liu, G. D. Samolyuk, Y. Lee, Ni Ni, T. Kondo, A. F. Santander-Syro, S. L. Bud'ko, J. L. McCesney, E. Rotenberg, T. Valla, A. V. Fedorov, P. C. Canfield, B. N. Harmon, and A. Kaminski,, Phys. Rev. Lett. **101**, 177005 (2008).

[12] H. Liu, W. Zhang, L. Zhao, X. Zia, J. Meng, G. Liu, X. Dong, G. F. Chen, J. L. Luo, N. L. Wang, W. Lu, G. Wang, Y. Zhou, Y. Zhu, X. Wang, Z. Xu, C. Chen, and X. J. Zhou, Phys. Rev. B **78**, 184514 (2008).

[13] L. Zhao, H.-Y. Liu, W.-T. Zhang, J.-Q. Meng, X.-W. Jia, G.-D. Liu, X.-Li. Dong, G.-F. Chen, J.-L. Luo, N.-L. Wang, L. Wei, G.-L. Wang, Y. Zhou, Y. Zhu, X.-Y. Wang, Z.-Y. Xu, C.-T. Chen, X.-J. Zhou, Chin. Phys. Lett. **25**, 4402 (2008).

[14] H. Ding, P. Richard, K. Nakayama, K. Sugawara, T. Arakane, Y. Sekiba, A. Takayama, S. Souma, T. Sato, T. Takahashi, Z. Wang, X. Dai, Z. Fang, G. F. Chen, J. L. Luo, and N. L. Wang, EPL **83**, 47001 (2008).

[15] V. B. Zabolotnyy, D. S. Inosov, D. V. Evtushinsky, A. Koitzsch, A. A. Kordyuk, G. L. Sun, J. T. Park, D. Haug, V. Hinkov, A. V. Horis, C. T. Lin, M. Knupfer, A. N. Yaresko, B. Büchner, A. Varykhalov, R. Follath, and S. V. Borinsenko, Nature (London) **457**, 569 (2009).

[16] H. Ding, K. Nakayama, P. Richard, S. Souma, T. Sato, T. Takahashi, M. Neupane, Y. Xu, Z. Pan, A. Federov, Z. Wang, X. Dat, Z. Fang, G. Chen, J. Luo, and N. Wang, arXiv:0812.0534 (unpublished).

[17] D. Hsieh, Y. Xia, L. Wray, D. Qian, K. Gomes, A. Yazdani, G. Chen, J. Luo, N. Wang, and M. Hasan, arXiv:0812.2289 (unpublished).

[18] Y. Sekiba, T. Sato, K. Nakayama, K. Terashima, P. Richard, J. H. Bowen, H. Ding, Y.-M. Xu, L. J. Li, G. H. Cao, Z.-A. Xu, and T. Takahashi, New J. Phys. **11**, 025020 (2009).

[19] D. H. Lu, M. Yi, S.-K. Mo, A. S. Erickson, J. Analytis, J.-H. Chu, D. J. Singh, Z. Hussain, T. H. Geballe, I. R. fisher, and Z.-X. Shen, Nature (London) **455**, 81 (2008).

[20] G. F. Chen, Z. Li, J. Dong, G. Li, W. Z. Hu, X. D. Zhang, X. H. Song, P. Zheng, N. L. Wang, and J. L. Luo, Phys. Rev. B **78**, 224512 (2008).

[21] The LDA calculations were done using the general potential linearized augmented plane-wave method, as in Ref. 9 but are on a more dense grid of k points to better show the details near the X point. Two different codes were used: an in-house code and the WIEN2K code, which were cross checked.

[22] Different photon energies probe the electronic structure at different k_z values, with 40 eV close to $k_z=\pi$ while 27 eV close to $k_z=0$.

[23] M. J. Calderon, B. Valenzuela, and E. Bascones, New J. Phys. **11**, 013051 (2009).

DISCLAIMER